Title	Stokes drift in equatorial water waves, and wave–current interactions
Authors	Henry, David
Publication date	2018-08-23
Original Citation	Henry, D. (2019) 'Stokes drift in equatorial water waves, and wave-current interactions', Deep Sea Research Part II: Topical Studies In Oceanography, 160, pp. 41-47. doi: 10.1016/j.dsr2.2018.08.003
Type of publication	Article (peer-reviewed)
Link to publisher's version	https://www.sciencedirect.com/science/article/pii/S0967064518301334 - 10.1016/j.dsr2.2018.08.003
Rights	© 2018 Elsevier Ltd. This manuscript version is made available under the CC-BY-NC-ND 4.0 license https://creativecommons.org/licenses/by-nc-nd/4.0/
Download date	2024-04-25 06:38:52
Item downloaded from	https://hdl.handle.net/10468/12185

Stokes drift in Equatorial water waves, and wave–current interactions

David Henry

Abstract

In this paper we review recent developments which enable the mathematical determination of various drift properties induced by water waves, and wave–current interactions, in the equatorial region. In particular, we describe results pertaining to a recently constructed exact solution of the geophysical fluid dynamic governing equations in the $\beta-$plane approximation at the Equator. The formulation of this exact solution renders it amenable to deriving an analytical expression for the Stokes' drift velocity, which is characterised in terms of the mean Eulerian flow velocity and the mean Lagrangian flow velocity. Additionally, an analysis of the associated mass transport is discussed. Notwithstanding the fact that the exact solution we discuss is in some sense a mathematical idealisation, from a physical perspective it may be regarded as a robust and reliable foundation on which to generate, and thereby model, more complex and intricate oceanographical flows.

1 Introduction

Determining the underlying fluid motion generated by water waves propagating on a free-surface is an intriguing and challenging area of oceanographical research which has important implications in the field (Constantin, 2011; Gill, 1982; Marshall and Plumb, 2016; Vallis, 2017). From a theoretical perspective, it is a subject of immense difficulty and complexity, with a paucity of fundamental research due to the intractability of the governing equations to mathematical analysis (Andrews and McIntyre, 1978; Bühler, 2009; Henry and Sastre-Gomez, 2016; Longuet-Higgins, 1953, 1969; van den Bremer and Breivik, 2018; Vallis, 2017). Accordingly, many investigations are pursued by way of observations from experiments and field data, although these approaches are themselves often perilous, cf. Monismith et al. 2007; Smith, 2006; van den Bremer and Breivik, 2018; Weber, 2011.

The origins of this area of oceanographical research may be traced to the observation of Stokes (1847) that fluid particles experience a mean net

drift velocity, in the direction of wave motion, when an average is taken over the wave period. Using purely formal mathematical considerations, Stokes illustrated that this fluid drift is an inherently nonlinear phenomenon which occurs at order ϵ^2, where ϵ relates to the wave steepness. At linear level, it had been classically assumed that particles undertake closed orbits. This presumption was founded on two main pillars, the first being a succession of mathematical approximations, whereby solutions of the linearised governing equations are themselves linearised, leading to apparently closed particle trajectories. The supposed closure of fluid particle orbits was then seemingly borne–out experimentally by extrapolating from highly-inconclusive photographs of fluid motion, such as those in van Dyke (1982). This tenet of classical fluid mechanics has been comprehensively debunked (Constantin, 2006,2011,2012a; Constantin et al., 2008; Constantin and Villari, 2008; Henry, 2006,2008b; Ionescu-Kruse, 2008; Lyons, 2014) using techniques from mathematical analysis which have proven that, both in the approximate linear regime, and for exact solutions of the fully nonlinear governing equations, particle paths throughout the fluid domain are uniformly non-closed. This is a striking, and recent, example of how a careful theoretical treatment can definitively, and conclusively, elucidate delicate physical processes which evade other, more applied, research approaches.

Furthermore, bearing in mind the overwhelming trend in physical oceanography of being guided primarily by numerical evidence and *ad-hoc* modelling, this example illustrates the relevance of pursuing theoretical investigations in oceanographical studies insofar as it is possible (Constantin and Johnson, 2016b; Johnson, 2018). In this review paper we describe developments, first presented in Henry and Sastre-Gomez (2016), which enable the mathematical determination of various drift properties induced by water waves, and wave–current interactions, in the equatorial region. In particular we describe results pertaining to the mean flow velocities, and related mass transport, induced by an exact solution to the geophysical fluid dynamics (GFD) governing equations in the $\beta-$plane approximation at the Equator. Geophysical processes which occur in the equatorial region are particularly fascinating from an oceanographical point of view (Constantin and Johnson, 2015; Cushman-Roisin and Beckers, 2011; Fedorov and Brown, 2009; Gill, 1982; Izumo, 2005; Johnson et al., 2001; Moum et al., 2011; Vallis, 2017). Physically, the equator acts as a natural wave guide whereby equatorially trapped zonal waves decay exponentially away from the equator.

From a general point of view, the mean fluid drift (or Stokes' drift) velocity can be characterised in terms of the mean Eulerian flow velocity and the mean Lagrangian flow velocity whereby: Lagrange = Euler + Stokes. Although the incorporation of Coriolis effects in the governing equations threatens to further obfuscate the already intractable nonlinear water wave problem, it transpires that the exact solution we analyse is amenable to an analysis of its mean flow velocities and related mass transport since it

assumes an explicit form in terms of Lagrangian variables.

In light of their scarcity, the existence of exact finite-amplitude solutions to the water wave problem is remarkable in itself— for two-dimensional gravity water waves the only known solution is Gerstner's wave (Constantin, 2001; Gerstner, 1809; Henry, 2008a; Stuhlmeier, 2015). While exact solutions in fluid dynamics are useful and important in their own right, in an oceanographical context they have the potential to be regarded as robust and reliable starting points to generate more physically realistic and observable flows by way of asymptotic, or multiple scale, methods. Such an undertaking promises to be technically challenging for the equatorial flows we consider here, and for discussions on the potential mathematical generalisations of exact solutions we defer to Constantin and Johnson (2016a,2017), Constantin and Monismith (2017), Henry (2016,2017), Johnson (2018), Mollo-Christensen (1978,1979) and Pollard (1970), and the references therein; an interesting discussion regarding the oceanographical relevance of the exact equatorial solutions being considered here can be found in Boyd (2018). The exact solution we analyse was first constructed in Henry (2013), and represents a generalised Gerstner-like solution of the GFD equations of the type which were initially derived in Constantin (2012,2013,2014). With the increase in structural complexity of the GFD governing equations, it is startling that the exact and explicit three-dimensional solutions described in Constantin (2012,2013,2014) and Henry (2013) exist, much less that they generalise Gerstner's wave (in the sense that, upon ignoring Coriolis terms, solutions reduce to two-dimensional gravity waves).

The exact solution we discuss comprises a (weakly) three-dimensional wave-like term which propagates periodically in the zonal direction with constant phasespeed $c > 0$, and the wave is equatorially trapped, exhibiting a strong exponential decay away from the Equator. A significant complicating factor for the theoretical analysis undertaken in this paper, particularly with regard to determining the mean Eulerian flow velocity and subsequently the Stokes drift velocity, is the presence of a depth-invariant underlying zonal current term in the solution presented in Henry (2013). This term assumes a deceptively simple manifestation in the Lagrangian formulation of the solution, yet it leads to significant complications, both mathematically and physically, in the resulting fluid motion. This is perhaps not surprising since the nonlinear passage from Lagrangian to Eulerian coordinates is a delicate issue in general (Bennett, 2006; Bühler, 2009; Constantin, 2011; Vallis, 2017). The incorporation of a depth-invariant underlying current in the wave-field kinematics is important from the perspective of future practical considerations, especially with regard to the potential for representing more physically realistic flows. This is particularly apposite since currents play a vital role in modelling the ocean's dynamics in the Equatorial region (Boyd, 2018; Cushman-Roisin and Beckers, 2011; Gill, 1982; Izumo, 2005; Johnson et al., 2001; Moum et al., 2011; Vallis, 2017).

2 Governing equations

The fully-nonlinear, exact governing equations for geophysical fluid dynamics on a rotating sphere, assuming the fluid is inviscid and incompressible (which are reasonable assumptions for ocean waves), take the form of the Euler equation

$$\frac{D\mathbf{u}}{Dt} + 2\mathbf{\Omega} \times \mathbf{u} + \mathbf{\Omega} \times (\mathbf{\Omega} \times \mathrm{r}) = -\frac{1}{\rho}\nabla P + \mathbf{F}, \tag{1}$$

together with the mass conservation equation

$$\nabla \cdot \mathbf{u} = 0. \tag{2}$$

The earth is assumed to be a perfect sphere of radius $R = 6378$ km, with $\mathbf{\Omega}$ the angular velocity vector of the earth's rotation (with $\Omega = 73 \times 10^{-6}$ rad/s the (constant) rotational speed). Here $\mathbf{u} = (u, v, w)$ is the fluid velocity field, D/Dt is the Lagrangian (or material) derivative, $\mathbf{F}$ is the external body force (in this model we assume $\mathbf{F}$ is solely gravitational), ρ is the water density (assumed to be constant), and P is the pressure. The second term in (1) is the Coriolis force, and the third term represents the centripetal force (which is typically neglected, although cf. Constantin and Johnson (2016a) and Henry (2016) for some interesting observations regarding the retention of this term).

Due to the complexity and intractability of the Euler equation (1) one typically invokes oceanographical considerations in order to derive simpler approximate models. The traditional $\beta-$plane model approximates the earth's curved surface (locally) by a tangent plane and is applicable when we restrict our focus to regions of relatively small latitudinal variation (around $2°$ either side of the equator). In the context of modelling equatorial flows the resulting (approximate) Euler equation takes the form

$$
\begin{aligned}
u_t + uu_x + vu_y + wu_z + 2\Omega w - \beta yv &= -\frac{1}{\rho}P_x \\
v_t + uv_x + vv_y + wv_z + \beta yu &= -\frac{1}{\rho}P_y \\
w_t + uw_x + vw_y + ww_z - 2\Omega u &= -\frac{1}{\rho}P_z - g,
\end{aligned}
\tag{3}
$$

where $\beta = 2\Omega/R = 2.28 \cdot 10^{-11}$ m^{-1}s^{-1}, and the origin of the $\{x, y, z\}-$ Cartesian coordinate reference frame is fixed at a point on the earth's surface at the equator, where the x-axis points horizontally due east (zonal), the y-axis due north (meridional), and the z-axis points vertically upwards perpendicular to the earth's surface.

The equations (3) above are of the "traditional β-plane approximation" form, which are ubiquitous in modelling equatorial flows. This formulation

arises from neglecting terms in the Coriolis force which feature the vertical velocity, and the vertical component of the Coriolis force. The approximation procedure which leads to (3) is not canonical, and there is quite a wide-array of research literature proposing alternative 'non-traditional' approximations which address various inconsistencies that arise in the classical approach, cf. the discussions in Constantin and Johnson (2016a,2017), Gerkema et al. (2008), Johnson (2018), Henry (2016,2017), Stewart and Dellar (2010), and the references therein. The equation (2) is expressed component-wise as

$$u_x + v_y + w_z = 0, \tag{4}$$

and for surface water waves the governing equations (3) and (4) are supplemented by the kinematic and dynamic surface boundary conditions

$$w = \eta_t + u\eta_x + v\eta_y \quad \text{on } z = \eta(x,y,t), \tag{5}$$

$$P = P_{atm} \quad \text{on } z = \eta(x,y,t), \tag{6}$$

where P_{atm} is the (constant) atmospheric pressure and $\eta(x,y,t)$ is the free-surface. Assuming the water to be infinitely deep, and converging with depth to a uniform underlying zonal current, results in the condition

$$(u,v,w) \to (-c_0,0,0) \quad \text{as } z \to -\infty. \tag{7}$$

If we wish to have no underlying depth-invariant current in the fluid flow we simply choose $c_0 = 0$, ensuring that there is no fluid motion at great depths.

3 Exact solution

The wave–current solution we analyse prescribes the Eulerian (reference frame) coordinates of fluid particles $(x(t), y(t), z(t))$ in terms of the Lagrangian labelling variables (q, r, s): a Lagrangian formulation considers the evolution in time of individual fluid particle motion (Bennett, 2006; Bühler, 2009; Constantin, 2011; Vallis, 2017). In Henry (2013) it was shown that the system

$$x = q - c_0 t - \frac{1}{k} e^{k[r-f(s)]} \sin[k(q-ct)], \tag{8a}$$

$$y = s, \tag{8b}$$

$$z = r + \frac{1}{k} e^{k[r-f(s)]} \cos[k(q-ct)], \tag{8c}$$

represents a solution of the $\beta-$plane governing equations (3) and (4), where $r \le r_0 < 0$ for a constant r_0, and k is the wavenumber defined by $k = 2\pi/L$, for L the (fixed) wavelength; field data examined in Moum et al. (2011) highlights the importance of waves with relatively short wavelengths (in the

range 150–250 m) for the dynamics of the upper-equatorial oceans. This solution (8) prescribes a (weakly) three-dimensional eastward-propagating steady geophysical wave in the presence of a constant underlying current of magnitude $|c_0|$. The wave-like term is periodic in the zonal direction and it has a constant phasespeed $c > 0$. If $c_0 > 0$ the underlying current is adverse, while for $c_0 < 0$ the current is following; $c_0 = 0$ corresponds to no underlying uniform current. Physically, the vanishing of the meridional component of the Coriolis force at the Equator has the effect that the Equator works as a (virtual) natural boundary, thereby facilitating azimuthal (zonal) flow propagation. The solution (8) exists mathematically for Lagrangian labelling variables $(q, r, s) \in (\mathbb{R}, (-\infty, r_0), \mathcal{I})$, where the sign of the current determines whether $\mathcal{I}$ is the real line $\mathbb{R}$ or a finite interval, as we discuss below. In physical terms, since the β-plane approximation results under the assumption that we are close to the equator we are *a priori* restricted to latitudes in the region $s \in [-s_0, s_0]$, where $s_0 = \sqrt{\tilde{c}/\beta} \approx 250$km is a typical value for the equatorial radius of deformation (and $\tilde{c}$ is a characteristic geophysical wavespeed, cf. Cushman-Roisin and Beckers, 2011) corresponding to (roughly) 2° latitude.

If we follow a "fixed" particle as the fluid motion evolves (that is, we fix the $(q, r, s)-$parameters) then particle trajectories are given by closed circles in a coordinate system moving with the underlying mean flow (which we take to be fixed if $c_0 = 0$). If $c_0 \neq 0$, then particles experience a net drift in the direction of c_0 and accordingly we expect there to be a non-zero mean Lagrangian velocity, as depicted in figure 1. It is interesting to note that, as opposed to the typical Eulerian framework, Lagrangian labelling variables do not necessarily represent the initial position of the particle they define; for instance, the parameters in (8) relate to the centre of the circle described by the particle motion.
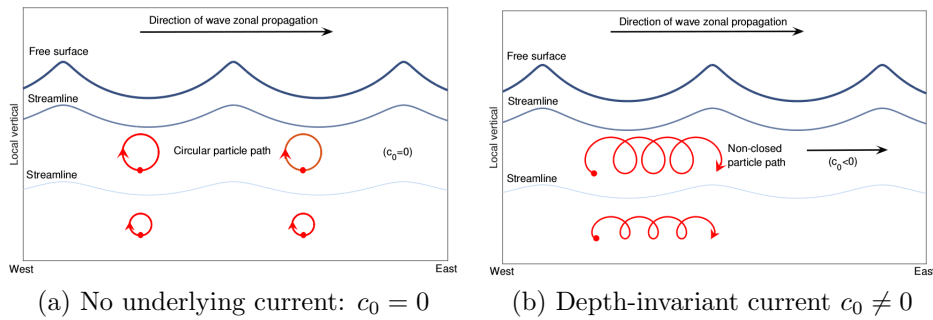

(a) No underlying current: $c_0 = 0$ (b) Depth-invariant current $c_0 \neq 0$

Figure 1: Depiction of the evolution of fixed fluid particles as prescribed by (8).

One of the pivotal steps in proving that the motion prescribed by (8) satisfies the Euler equation (3) is the construction of a suitable pressure

distribution function. It transpires that the appropriate choice is given by

$$P = \rho\gamma\left(\frac{e^{2\xi}}{2k} - r + \frac{c_0}{c}f(s)\right) + P_{atm} - \rho g\left(\frac{e^{2kr_0}}{2k} - r_0\right). \qquad (9)$$

The function $f(s)$ determines the meridional decay of the particle oscillations away from the equator and must be given by

$$f(s) = \frac{c\beta}{2\gamma}s^2, \qquad (10)$$

where $\gamma = 2\Omega c_0 + g$ is a "modified gravity" term: we make the physical assumption that $\gamma > 0$, since $g/2\Omega \approx 6.7 \times 10^4\,\mathrm{m\,s^{-1}}$. At fixed-latitudes $y = s$, we let $r(s) < r_0$ denote the unique solution of the equation

$$\frac{e^{2k[r(s) - \frac{c\beta}{2\gamma}s^2]}}{2k} - r(s) + \frac{c_0\beta}{2\gamma}s^2 - \frac{e^{2kr_0}}{2k} + r_0 = 0. \qquad (11)$$

The free-surface $z = \eta(x, s, t)$ at this latitude is then implicitly prescribed by setting $r = r(s)$ in (8c). For a given current c_0, in order that a unique solution of (11) exists it is necessary that

$$c_0 < ce^{2kr_0}. \qquad (12)$$

For $c_0 \leq 0$, (11) has a solution for all $s \in \mathbb{R}$, whereas for $c_0 > 0$ we observe from (12) that (11) can only be solved for a restricted range of values of $s \in \mathcal{I}$, where the size of $\mathcal{I}$ depends on the current's magnitude. We note that for wavelengths in the range $150 - 250$m, condition (12) holds at the equator for all physically reasonable values of the underlying current c_0, as we describe in Remark 3 below. Examining the forms of relations (9) and (11) we see that the surface dynamic boundary condition (6) holds by construction. Furthermore, the structure of the solution (8), coupled with this prescription method for the free-surface $z = \eta(x, y, t)$, ensures that the kinematic surface condition (5) also holds: all particles originating on the wave surface will remain at the surface for all time. The form of (10) ensures that the wave is Equatorially trapped, exhibiting a strong exponential decay away from the Equator. The steepness of the resulting wave profile, defined to be half the amplitude multiplied by the wavenumber, can be expressed as

$$\tau(s) = e^{k(r - f(s))},$$

which is maximised by the value $\tau_0 = e^{kr_0}$ attained at the equator. To illustrate typical values of the maximum steepness we take $r_0 = -20$m, for example; this then gives us a value of $\tau_0 = 0.43$ for a wavelength of $L = 150$m, whereas for wavelengths of $L = 250$m we have $\tau_0 = 0.6$. Furthermore, at each fixed-latitude $y = s$ in a coordinate system moving with the mean

7

flow (which we take to be fixed if $c_0 = 0$), the free-surface is an inverted trochoid (cf. Constantin, 2011) and particle trajectories take the form of closed circles as depicted in figure 2. In the limiting case $r_0 \to 0$ the free-surface approaches a cycloid at the equator ($s = 0$), exhibiting the associated singular cusps at the crests (Constantin, 2011).
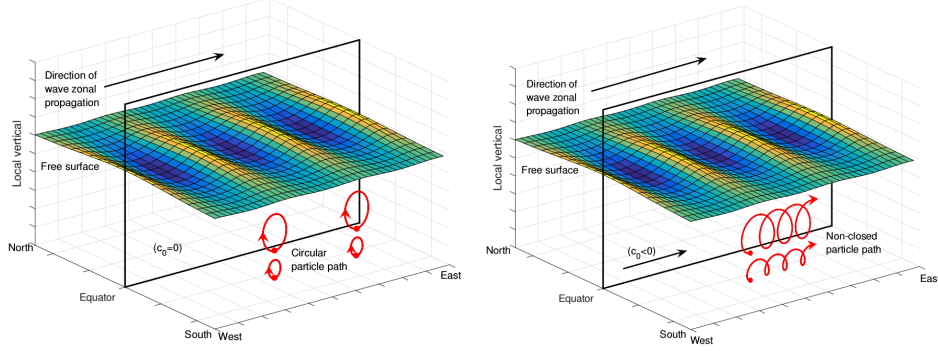

Figure 2: Depiction of the equatorially-trapped trochoidal free-surface wave

One appreciable benefit of working in the Lagrangian framework is that fluid kinematics can often be described with relative ease and, in our case, explicitly since the solution (8) is prescribed explicitly in the Lagrangian formulation. The velocity field is calculated directly from (8) to get

$$u(q, r, s; t) = \frac{Dx}{Dt} = ce^{k(r-f(s))} \cos k(q - ct) - c_0, \tag{13a}$$

$$v(q, r, s; t) = \frac{Dy}{Dt} = 0, \tag{13b}$$

$$w(q, r, s; t) = \frac{Dz}{Dt} = ce^{k(r-f(s))} \sin k(q - ct). \tag{13c}$$

Regarding the flow prescribed by (13), equatorial field data (see Johnson et al., 2001) confirms the fact that meridional speeds near the Equator are much smaller than the zonal speeds, and neglecting them, as the prescribed fluid motion (8) and (13) does, therefore has an insignificant dynamical effect. Accordingly, wave patterns of the type predicted by our considerations are relevant to the dynamics of the ocean in the equatorial Pacific. The flow prescribed by (8) and (13) is rotational, as is expected for geophysical water waves, with the (weakly) three-dimensional vorticity computed as

$$\boldsymbol{\omega} = \left(-s\frac{kc^2\beta}{g} \frac{e^\xi \sin\theta}{1 - e^{2\xi}}, -\frac{2kce^{2\xi}}{1 - e^{2\xi}}, s\frac{kc^2\beta}{g} \frac{e^\xi \cos\theta - e^{2\xi}}{1 - e^{2\xi}} \right),$$

where we denote $\xi = k(r - f(s))$, $\theta = k(q - ct)$. As a by-product of the derivation of (9) we obtain the dispersion relation for the wave phase-speed,

$$c = \frac{\sqrt{\Omega^2 + k\gamma} - \Omega}{k} = \frac{\sqrt{\Omega^2 + k(2\Omega c_0 + g)} - \Omega}{k} > 0, \tag{14}$$

which details the effect that the rotational and current terms have on the wavespeed; setting $\Omega = c_0 = 0$ recovers the dispersion relation $c = \sqrt{g/k}$ for Gerstner (and deep-water gravity) waves.

Remark 1 We note that the dispersion relation (14) gives a wavespeed $c \approx 15\,\mathrm{m\,s}^{-1}$ for a wave of length $L = 150$m, whereas $c \approx 19.7\,\mathrm{m\,s}^{-1}$ for waves of length 250m. In particular, for these values the right-hand side of relation (12) is $2.8\,\mathrm{m\,s}^{-1}$, and $7.2\,\mathrm{m\,s}^{-1}$, respectively. Bearing in mind that equatorial currents typically have a magnitude less than $1\,\mathrm{m\,s}^{-1}$ (Gill, 1982), it follows that we expect condition (12) to hold at the equator for physically reasonable values of the underlying current c_0.

4   Stokes drift

The Stokes drift (or mean Stokes flow velocity), which is the difference between the mean Lagrangian and Eulerian velocities (Longuet-Higgins, 1953, 1969), is eastwards in the absence of the current ($c_0 = 0$). Indeed, it was shown in Constantin and Germain (2013) that in this setting the mean Lagrangian velocity is zero and the mean Eulerian velocity flows westwards. It is perhaps not surprising that the situation is far more complex with the incorporation of a constant underlying current, in particular with regard to determining the mean Eulerian velocity, as we now describe. Throughout the following considerations we fix the latitude by setting $s = s_*$, and we note that at fixed latitudes $s = s_*$ the crest and trough levels of the wave surface profile are prescribed in terms of the Lagrangian parameters by

$$z_\pm(s_*) = r_0(s_*) \pm \frac{1}{k}e^{k[r_0(s_*) - f(s_*)]}.$$

4.1   Mean Lagrangian velocity

The mean Lagrangian flow velocity, also known as the mass-transport velocity (Longuet-Higgins, 1969), at a point in the fluid domain is the mean velocity over a wave period of a marked fluid particle which originates at that point. For flows prescribed by (8) the wave–averaged zonal velocity is

$$\langle u \rangle_L = \frac{1}{T}\int_0^T u(q - ct, s_*, r)dt = \frac{ce^\xi}{T}\int_0^T \cos\left[k(q - ct)\right]dt - \frac{1}{T}\int_0^T c_0\,dt = -c_0.$$

(15)

Hence, depending on the sign of c_0, the mean Lagrangian flow velocity is either westwards or eastwards; when $c_0 = 0$ the mean Lagrangian velocity is zero. The expression for the mean Lagrangian velocity is independent of both the latitude s_*, and the location from where the fluid parcel originates.

4.2 Mean Eulerian velocity

Fixing a point in space at a depth beneath the wave-trough level, the mean Eulerian flow velocity is the average of the Eulerian fluid velocity (over a wave-period) at that point. For the velocity field (13) the mean Eulerian flow velocity is given by the mean of the horizontal velocity. Letting $z = z_-(s_*)$ denote the vertical position of the wave trough level, we fix a depth $z = z_0 < z_-(s_*)$. The equation

$$z_0 = R + \frac{1}{k} e^{\xi(R)} \cos\theta \tag{16}$$

then induces a functional relationship between the erstwhile independent variables r and q, which we denote by $r = R(q - ct; s_*, z_0)$. For a given fixed-depth z_0, the maximal and minimal values achieved by R are determined implicitly by the relations

$$z_0 = R \pm \frac{1}{k} e^{\xi(R)},$$

where the positive (negative) sign corresponds to the minimal (maximal) value of R, respectively. Following a number of computations it transpires that the mean Eulerian velocity takes the form

$$\langle u \rangle_E(s_*, z_0) \;\; = -\frac{c}{L} \int_0^L e^{2\xi(R(q))} dq - \frac{c_0}{L} \int_0^L \frac{1 - e^{2\xi(R(q))}}{1 + e^{\xi(R(q))} \cos(k[q - ct])} dq. \tag{17}$$

It is clear from the above expression that a non-zero depth invariant current c_0 adds significant complications in computing the mean Eulerian velocity (17): in particular the sign (and hence direction) of the mean Eulerian velocity is not easily discernible from the above expression in general. Nevertheless, depending on the size and direction of the current c_0, the inequalities

$$\int_0^L \frac{1 - e^{2\xi}}{1 + e^\xi} dq \leq \int_0^L \frac{1 - e^{2\xi}}{1 + e^\xi \cos\theta} dq \leq \int_0^L \frac{1 - e^{2\xi}}{1 - e^\xi} dq \tag{18}$$

lead to estimates which can be employed to determine the direction of the mean Eulerian velocity.

For an adverse underlying current, $c_0 > 0$, we note that condition (12) provides the restriction $0 < c_0 < ce^{2kr_0} < c$. Since $\xi \leq kR < kr_0 < 0$, for all latitudes s and depths $z_0 < z_-(s)$, we deduce that the mean Eulerian flow velocity must lie in the range

$$\langle u \rangle_E(s, z_0) \in \left(-c\frac{1 - e^{3kr_0}}{1 - e^{kr_0}}, 0 \right). \tag{19}$$

That the mean Eulerian flow is westward for an adverse current is not surprising, since in the absence of the current the mean Eulerian flow is westwards, cf. Constantin and Germain (2013).

For the case of a following underlying current, $c_0 \leq 0$, the influence that the underlying current has on the mean Eulerian flow in (17) is even more difficult to ascertain, and it is not possible to determine its effect directly. Nevertheless, we deduce from (17) that the mean Eulerian velocity is westwards, that is $\langle u \rangle_E(s_*, z_0) < 0$, if

$$c_0 > -c \min_{q \in [0,L]} \frac{e^{2k(R(q;z_0)-f(s_*))}\left(1 - e^{k(R(q;z_0)-f(s_*))}\right)}{1 - e^{2k(R(q;z_0)-f(s_*))}}, \qquad (20)$$

and the mean Eulerian flow (17) is eastwards, $\langle u \rangle_E(s_*, z_0) > 0$, if

$$c_0 < -c \max_{q \in [0,L]} \frac{e^{2k(R(q;z_0)-f(s_*))}\left(1 + e^{k(R(q;z_0)-f(s_*))}\right)}{1 - e^{2k(R(q;z_0)-f(s_*))}}. \qquad (21)$$

These expressions, while admittedly convoluted in appearance, are nevertheless in a form which should be prove amenable to numerical computation for given data values. In the absence of an underlying current ($c_0 = 0$) condition (20) always holds and so the resulting mean Eulerian velocity is in the westerly direction, as first observed in Constantin and Germain (2013).

4.3   Stokes drift

The Stokes drift (or mean Stokes) velocity $U^S(z_0)$ is defined by the relation

$$\langle u \rangle_L(z_0) = \langle u \rangle_E(z_0) + U^S(z_0),$$

and for the flow defined by (8) it takes the form

$$U^S = \langle u \rangle_L - \langle u \rangle_E$$
$$= \frac{c}{L} \int_0^L e^{2\xi(R(q))} dq + \frac{c_0}{L} \int_0^L \frac{1 - e^{2\xi(R(q))}}{1 + e^{\xi(R(q))} \cos\left(k\left[q - ct\right]\right)} dq - c_0. \qquad (22)$$

For an adverse current, $c_0 \geq 0$, it follows immediately from (22) and (12) that

$$U^S = \frac{1}{L} \int_0^L \left(c e^{2\xi(R(q))} - c_0\right) dq + \frac{c_0}{L} \int_0^L \frac{1 - e^{2\xi(R(q))}}{1 + e^{\xi(R(q))} \cos\left(k\left[q - ct\right]\right)} dq > 0.$$

Therefore for $c_0 \geq 0$ the Stokes drift is eastwards throughout the fluid domain. In the case of a following current, $c_0 < 0$, the expression for Stokes drift (22) is not easily discerned, in general, from direct inspection (although it is expected that expression (22) will prove responsive to numerical approaches). Nevertheless, if the magnitude of the current is such that (21) holds then we can conclude that the Stokes drift is westwards.

5   Mass flux

Since the Lagrangian velocity is the wave-averaged velocity of a marked particle, it is sometimes called the mass-transport velocity. For a non-zero underlying current, $c_0 \neq 0$, it is clear that the total mass flux induced by (8) below the free-surface wave past a point $x = x_0$, which is fixed in Eulerian coordinates, will be infinite. Of greater interest is the consideration of the mass-flux past a point x_0 which is fixed in a frame moving with speed c_0: this is equivalent to considering the situation $c_0 = 0$ in (8). The total mass-transport beneath the surface wave is given by the integral

$$m(x_0 - ct, s) = \int_{-\infty}^{\eta(x_0 - ct, s)} u(x_0 - ct, s, z) dz. \tag{23}$$

In order to cast (23) in terms of the Lagrangian labelling variables we induce a functional relationship between q and the variables r, t, denoted by $q = \gamma(r, t; s_*)$, by way of fixing $x = x_0$ in the expression

$$x_0 = q - \frac{1}{k} e^\xi \sin \theta.$$

Differentiating the above expression with respect to r gives

$$0 = \gamma_r - e^\xi \sin \theta - \gamma_r e^\xi \cos \theta,$$

and so

$$\frac{dz}{dr} = 1 + e^\xi \cos \theta - \gamma_r e^\xi \sin \theta = \frac{1 - e^{2\xi}}{1 - e^\xi \cos \theta},$$

where we have used the relation

$$\gamma_r = \frac{e^\xi \sin \theta}{1 - e^\xi \cos \theta}.$$

Therefore we have

$$
\begin{aligned}
m(x_0 - ct, s) &= \int_{-\infty}^{r_0} (ce^\xi \cos \theta) \frac{dz}{dr} dr \\
&= \int_{-\infty}^{r_0} (ce^\xi \cos \theta) \frac{1 - e^{2\xi}}{1 - e^\xi \cos \theta} dr.
\end{aligned}
\tag{24}
$$

Although the integral in (24) is over an infinite range, this is balanced by the fact that terms involving ξ decay exponentially as $r \to -\infty$. It follows from (8a) (with $c_0 = 0$) that the function γ is $T-$periodic, and furthermore differentiating (8a) with respect to t yields

$$\gamma_t = \frac{-ce^\xi \cos \theta}{1 - e^\xi \cos \theta}. \tag{25}$$

Combining (24) and (25) we observe that the mass flux is given by

$$m(x_0 - ct, s) = \int_{-\infty}^{r_0} -\gamma_t(1 - e^{2\xi})dr,$$

and since γ is $T-$periodic it follows immediately that the average of the mass flux over a period T is zero. In the case where c_0 is non-zero we may still deduce mass-flow properties in a finite region near the free-surface. If the magnitude of the current c_0 is such that

$$|c_0| \leq ce^{k(\tilde{r}(s_*) - f(s_*))}, \tag{26}$$

where the value $\tilde{r}(s_*) < r_0(s_*)$ denotes some streamline beneath the surface, then the expression

$$\tilde{m}(x_0 - ct, s) \quad = \int_{\tilde{r}}^{r_0} (-c_0 + ce^{\xi}\cos\theta)\frac{1 - e^{2\xi}}{1 - e^{\xi}\cos\theta}dr, \tag{27}$$

implies that the mass flux between $\tilde{r}$ and r_0 is positive at the crest and negative at the trough. Therefore, for currents sufficiently small that (26) holds, and in regions close to the surface between $\tilde{r}$ and r_0, at the crest the mass flux (27) is forward and at the trough the mass flux goes backward, matching the properties of the flows observed in Constantin and Germain (2013) and Longuet-Higgins (1969) and depicted in Figure 3 below. We note that, using the reference value $c_0 = 1\,\mathrm{m\,s}^{-1}$ (which corresponds to the maximal typical equatorial current magnitude, cf. Gill (1984)) and the physical values discussed in Remark 1, we infer that condition (26) holds for $\tilde{r}(s_*) \gtrapprox -64$m in the case of waves of length 150m, whereas for wavelengths of 250m condition (26) holds for $\tilde{r}(s_*) \gtrapprox -118$m.
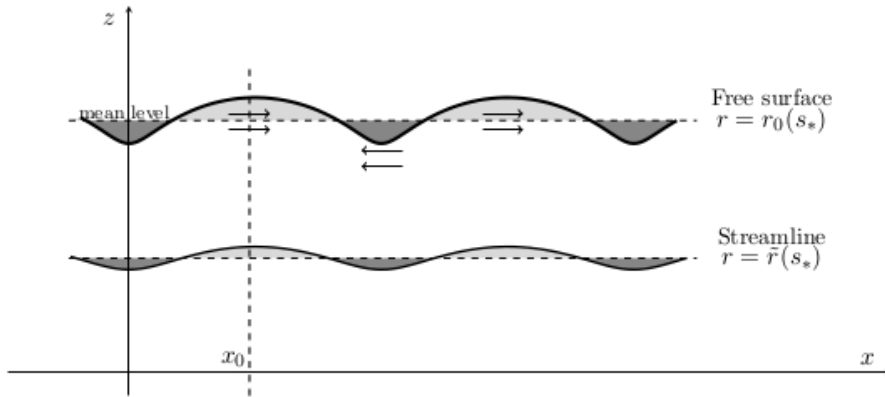

Figure 3: Behaviour of the mass-flux between the free-surface $r = r_0(s_*)$ and streamline $r = \tilde{r}(s_*)$

The behaviour is markedly different in the case where $c_0 < -ce^{k(\tilde{r}(s_*)-f(s_*))}$. Here the mass-flux between $\tilde{r}$ and r_0 (given by (27)) at the crest is forwards, as expected, however at the trough the mass-flux is also forwards: this anomalous behaviour is explained solely by the presence of the constant underlying current.

6 Discussions

The above considerations outline how we can employ a mathematical approach to determine drift properties which are induced by water waves, and wave–current interactions, in the equatorial region. While the exact solution (8) we have analysed is an idealised flow, from a physical perspective, it is clear from the discussions that the wave–current interactions prescribed by this solution possess some of the structure observed in field data for equatorial flows, at least in the region which is suitably described by the traditional $\beta-$plane approximation (around $2°$ each side of the equator).

With this in mind, and with regard to their relevance in future mathematical investigations of oceanographical phenomena, we reiterate the assertion that exact solutions represent a robust and reliable foundation on which to potentially construct more physically realistic and observable flows, and it is hoped that the above presentation has expounded how a careful theoretical treatment can elucidate the delicate physical processes underlying fluid motions, which otherwise evade alternative, more applied, research approaches. The robustness and adaptability of exact Gerstner-like solutions in describing Equatorial water waves is further exemplified by the fact that such solutions exist for non-traditional $\beta-$plane governing equations, which retain centripetal forces (cf. Henry (2016)), and incorporate the geometry of the earth's curvature (cf. Henry (2017)), respectively.

This paper has focussed on surface wave flows, but we remark that exact and explicit Langrangian solutions representing Equatorially-trapped internal waves were constructed in Constantin (2013,2014), with underlying currents incorporated in Kluczek (2017), Rodríguez-Sanjurjo (2017) and Rodríguez-Sanjurjo and Kluczek (2017); these papers contain a mathematically analogous analysis of the mean-flow properties yielding physically quite different results.

Additionally, we remark that while geophysical processes which occur in the equatorial region are particularly fascinating from an oceanographical point of view, it would be interesting, and very useful, to seek exact and explicit solutions which exist at mid-latitudes. In Pollard (1970), a nonlinear geophysical wave solution was constructed which can exists at mid-latitudes, and recently in Constantin and Monismith (2017) the authors accommodate a depth-invariant current into this solution. From the perspective whereby exact solutions may help us gain insight into the structure of the GFD gov-

erning equations, it is remarkable that the presence of the underlying current in Constantin and Monismith (2017) serves to generate a new slow-mode representing an inertial Gerstner wave, which is a fundamentally nonlinear phenomenon in which very small free surface deflections are manifestations of an energetic current. This striking, newly-derived wave solution serves to further illustrate the power, and relevance, of pursuing theoretical investigations in oceanographical studies. This work has yet to be investigated from the viewpoint of the Stokes' drift phenomena, and an interesting extension would be to try to construct Pollard-like internal wave solutions.

Finally, potential future investigations of Stokes' drift might include an element of continuous stratification into the fluid prescription. Stratification is ubiquitous in geophysical fluid dynamics, and particularly so for equatorial dynamics where there is a pronounced thermocline. The thermocline is most commonly represented as an interface separating two homogeneous fluid layers possessing a discrete (yet small) jump in densities. It is noteworthy that wave propagation on the thermocline may be modelled by the internal wave solutions mentioned above. In relation to continuously stratified fluids, note that variable density may be accommodated in the fluid model presented in this paper in the absence of an underlying current ($c_0 = 0$). This is effected through introducing an additional equation of motion,

$$\rho_t + u\rho_x + v\rho_y + w\rho_z = 0,$$

which must be satisfied to ensure conservation of mass. Prescribing the density function by

$$\rho(r, s) = F\left(\frac{e^{2\xi}}{2k} - r\right), \tag{28}$$

where $F : (0, \infty) \to (0, \infty)$ is continuously differentiable and non-decreasing, the analogue of the pressure function (9) is given, where $\mathcal{F}' = F$ and $\mathcal{F}(0) = 0$, by

$$P = g\mathcal{F}\left(\frac{e^{2\xi}}{2k} - r\right) + P_{atm} - g\mathcal{F}\left(\frac{e^{2kr_0}}{2k} - r_0\right).$$

The incorporation of continuous stratification promises to greatly complicate issues relating to mass-transport, in particular, the description of which has profound implications for attaining a detailed understanding of the oceanographical processes underlying geophysical fluid dynamics.

Acknowledgements

References

Andrews, D. G. and McIntyre, M. E., 1978. An exact theory of waves on a Lagrangian mean flow. *J. Fluid Mech.* **89**, 609–646.

Bennett A. 2006 *Lagrangian fluid dynamics*, Cambridge University Press, Cambridge.

Boyd J. P. 2018. *Dynamics of the Equatorial Ocean*, Springer, Berlin.

Bühler, O. 2009 *Waves and Mean Flows*. Cambridge University Press, Cambridge.

Constantin A. 2001 On the deep water wave motion *J. Phys. A* **34**, 1405–1417.

Constantin A. 2006 The trajectories of particles in Stokes waves, *Invent. Math.* **166**, 523–535.

Constantin A. 2011 *Nonlinear Water Waves with Applications to Wave-Current Interactions and Tsunamis*, CBMS-NSF Conference Series in Applied Mathematics, Vol. 81, SIAM, Philadelphia.

Constantin, A. 2012. Particle trajectories in extreme Stokes waves, *IMA J. Appl. Math.* **77**, 293–307.

Constantin, A. 2012 An exact solution for equatorially trapped waves, *J. Geophys. Res.: Oceans* **117** C05029.

Constantin A. 2013 Some three-dimensional nonlinear Equatorial flows, *J. Phys. Oceanogr.* **43**, 165–175.

Constantin A. 2014 Some nonlinear, Equatorially trapped, nonhydrostatic internal geophysical waves, *J. Phys. Oceanogr.* **44**, 781–789.

Constantin, A., Ehrnström, M. and Villari, G. 2008. Particle trajectories in linear deep-water waves. *Nonlinear Anal. Real World Appl.* **9**, 1336–1344.

Constantin A. and Germain P. 2013 Instability of some Equatorially trapped waves, *J. Geophys. Res.: Oceans* **118**, 2802–2810.

Constantin A. and Johnson R. S. 2015 The dynamics of waves interacting with the Equatorial Undercurrent, *Geophys. Astrophys. Fluid Dyn.* **109**, 311–358.

Constantin A. and Johnson R. S. 2016 An exact, steady, purely azimuthal equatorial flow with a free surface, *J. Phys. Oceanogr.* **46**, 1935–1945.

Constantin A. and Johnson R. S. 2016 Current and future prospects for the application of systematic theoretical methods to the study of problems in physical oceanography *Phys. Lett. A* **380** 3007–3012.

Constantin A. and Johnson R. S. 2017 A nonlinear, three-dimensional model for ocean flows, motivated by some observations of the Pacific Equatorial Undercurrent and thermocline, *Phys. Fluids* **29** 056604.

Constantin A. and Monismith S.G. 2017 Gerstner waves in the presence of mean currents and rotation *J. Fluid Mech.* **820** 511–528.

Constantin, A. and Villari, G. 2008. Particle trajectories in linear water waves. *J. Math. Fluid Mech.* **10**, 1–18.

Cushman-Roisin B. and Beckers J.-M. 2011 *Introduction to Geophysical Fluid Dynamics: Physical and Numerical Aspects*, Academic, Waltham, Mass..

Fedorov A. V. and Brown J. N. 2009 Equatorial waves, in *Encyclopedia of Ocean Sciences*, edited by J. Steele, pp. 3679–3695, Academic, San Diego, Calif..

Gerkema T., Zimmerman J.T.F., Maas L.R.M. and van Haren H. 2008. Geophysical and astrophysical fluid dynamics beyond the traditional approximation. *Rev. Geophys.* **46**, RG2004.

Gerstner, F. 1809. Theorie der Wellen samt einer daraus abgeleiteten Theorie der Deichprofile. *Ann. Phys. 2*, 412–445.

Gill A. 1982 *Atmosphere-ocean dynamics*, Academic Press, New York.

Henry, D. 2006. The trajectories of particles in deep-water Stokes waves, *Int. Math. Res. Not.* 13. Art. ID 23405.

Henry D. 2008 On Gerstner's water wave, *J. Nonl. Math. Phys.* **15**, 87–95.

Henry D. 2008 On the deep-water Stokes flow, *Int. Math. Res. Not.* **22**, Art. 071.

Henry D. 2013 An exact solution for equatorial geophysical water waves with an underlying current, *Eur. J. Mech. B Fluids* **38**, 18–21.

Henry D. 2016 Equatorially trapped nonlinear water waves in a $\beta-$plane approximation with centripetal forces, *J. Fluid Mech.* **804** R1.

Henry D. 2017 A modified equatorial $\beta-$plane approximation modelling nonlinear wave-current interactions, *J. Diff. Eq.* **263** 2554-2566.

Henry D. and Sastre-Gómez S. 2016 Mean flow velocities and mass transport for Equatorially-trapped water waves with an underlying current, *J. Math. Fluid Mech.* **18** 795–804.

Ionescu-Kruse D. 2008. Particle trajectories in linearized irrotational shallow water flows, *J. Nonlinear Math. Phys.* **15**, 13–27.

Izumo T. 2005 The equatorial current, meridional overturning circulation, and their roles in mass and heat exchanges during the El Niño events in the tropical Pacific Ocean, *Ocean Dyn.*, **55**, 110–123.

Johnson G. C., McPhaden M. J. and Firing E. 2001, Equatorial Pacific ocean horizontal velocity, divergence, and upwelling, *J. Phys. Oceanogr.* **31**, 839–849.

Johnson R.S. 2018 Application of the ideas and techniques of classical fluid mechanics to some problems in physical oceanography, *Phil. Trans. R. Soc. A* **276**, 20170092

Kluczek M. 2017 Exact and explicit internal equatorially-trapped water waves with underlying currents. *J. Math. Fluid Mech.* **19**, 305–314.

Longuet-Higgins, M. S. 1953. Mass transport in water waves, *Philos. Trans. R. Soc. Lond. A* **245** 535–581.

Longuet-Higgins M.S. 1969 On the transport of mass by time-varying ocean currents, *Deep Sea Res.* **16**, 431–447.

Lyons T. 2014 Particle trajectories in extreme Stokes waves over infinite depth. *Discrete Contin. Dyn. Syst.* **34**, 3095–3107.

Marshall J. and Plumb R. A., 2016. *Atmosphere, ocean and climate dynamics: an introductory text*. Academic Press.

Mollo-Christensen E. 1978 Gravitational and Geostrophic Billows: Some Exact Solutions, *J. Atmos. Sci.* **35**, 1395–1398.

Mollo-Christensen E. 1979 Edge waves in a rotating stratified fluid, an exact solution, *J. Phys. Ocean.* **9**, 226–229.

Monismith S.G., Cowen E.A., Nepf H.M., Magnaudet J. and Thais L. 2007 Laboratory observations of mean flow under surface gravity waves, *J. Fluid Mech.* **573**, 131–147.

Moum J. N., Nash, J. D. and Smyth W. D. 2011 Narrowband oscillations in the upper equatorial ocean. Part I: Interpretation as shear instability, *J. Phys. Oceanogr.* **41**, 397–411.

Pollard R.T. 1970 Surface waves with rotation: An exact solution, *J. Geophys. Res.* **75** 5895–5898.

Rodríguez-Sanjurjo A. 2017 Internal equatorial water waves and wave–current interactions in the $f-$plane. *Monatsh. Math.* DOI 10.1007/s00605-017-1052-z.

Rodríguez-Sanjurjo A. and Kluczek M. 2017 Mean flow properties for equatorially trapped internal water wave–current interactions *Appl. Anal.* **96** (2017), 2333–2345.

Smith, J. A. 2006. Observed variability of ocean wave Stokes drift, and the Eulerian response to passing groups. *J. Phys. Oceanogr.* **36**, 1381–1402.

Stewart A. L. and Dellar, P. J. 2010 Multilayer shallow water equations with complete Coriolis force. Part I: Derivation on a non-traditional beta-plane, *J. Fluid Mech.* **651**, 387–413.

Stokes, G.G. 1847. On the theory of oscillatory waves, *Trans. Camb. Phil. Soc.* **8**, 441–445.

Stuhlmeier R. 2015. On Gerstner's water wave and mass transport, *J. Math. Fluid. Mech.*, **17**, 761–767.

Vallis G. K. 2017 *Atmospheric and Oceanic Fluid Dynamics*, 2nd ed., Cambridge University Press.

van den Bremer, T. S. and Breivik, O. 2018. Stokes drift. *Philos. Trans. Roy. Soc. A* **376**, 20170104.

van Dyke, M. 1982 *An album of fluid motion.* The Parabolic Press, Stanford, USA.

Weber J.E.H. 2011 Do we observe Gerstner waves in wave tank experiments? *Wave Motion* **48**, 301–309.